



## Search for a $t\bar{t}$ Resonance in $p\bar{p}$ Collisions at $\sqrt{s} = 1.96$ TeV in the Lepton+Jets Final State

The DØ Collaboration  
URL <http://www-d0.fnal.gov>  
(Dated: August 16, 2005)

A search for a narrow-width heavy resonance decaying into top quark pairs ( $X \rightarrow t\bar{t}$ ) in  $p\bar{p}$  collisions at  $\sqrt{s} = 1.96$  TeV has been performed using data collected by the DØ detector at the Fermilab Tevatron collider. This analysis considers  $t\bar{t}$  candidate events in the lepton+jets channel using a lifetime tag to identify  $b$ -jets and the  $t\bar{t}$  invariant mass distribution to search for evidence of resonant production. The analyzed dataset corresponds to an integrated luminosity of approximately  $370 \text{ pb}^{-1}$ . We find no evidence for a  $t\bar{t}$  resonance  $X$ , therefore we set upper limits on  $\sigma_X \times B(X \rightarrow t\bar{t})$  for different hypothesized resonance masses using a Bayesian approach. Within a topcolor-assisted technicolor model, the existence of a leptophobic  $Z'$  boson with  $M_{Z'} < 680$  GeV and width  $\Gamma_{Z'} = 0.012M_{Z'}$  can be excluded at 95% C.L..

## I. INTRODUCTION

The top quark has by far the largest mass of all known elementary particles. This suggests that the top quark may play a special role in the dynamics of electroweak symmetry breaking. One of the various models incorporating this possibility is topcolor [1], where the large top quark mass can be generated through a dynamical  $t\bar{t}$  condensate,  $X$ , which is formed by a new strong gauge force preferentially coupled to the third generation of fermions. In one particular model, topcolor-assisted technicolor [2],  $X$  couples weakly and symmetrically to the first and second generations and strongly to the third generation of quarks, and has no couplings to leptons, resulting in a predicted cross section for  $t\bar{t}$  production larger than the standard model (SM) prediction.

In this analysis a model-independent search for a narrow-width heavy resonance  $X$  decaying into  $t\bar{t}$  is performed. In the framework of the SM, the top quark decays into a  $W$  boson and  $b$  quark nearly 100% of the time. The  $t\bar{t}$  event signature is fully determined by the  $W$  boson decay modes. In this analysis only the lepton+jets ( $\ell$ +jets, where  $\ell = e$  or  $\mu$ ) final state, which results from the leptonic decay of one of the  $W$  bosons and the hadronic decay of the other, is considered. The event signature is one isolated electron or muon with high transverse momentum ( $p_T$ ), large transverse energy imbalance ( $\cancel{E}_T$ ) due to the undetected neutrino, and at least four jets, two of which result from the hadronization of the  $b$  quarks.

The analyzed dataset corresponds to an integrated luminosity of  $366 \pm 24 \text{ pb}^{-1}$  in the  $e$ +jets channel and  $363 \pm 24 \text{ pb}^{-1}$  in the  $\mu$ +jets channel, collected between August 2002 and August 2004. The signal-to-background ratio is improved by identifying  $b$ -jets using a lifetime based  $b$ -tagging algorithm. After  $b$ -tagging, the dominant physics background for a resonance signal is non-resonant SM  $t\bar{t}$  production. Smaller contributions arise from the direct production of  $W$  bosons in association with four or more jets ( $W$ +jets), as well as instrumental background originating from multijet processes with jets faking isolated leptons. The search for resonant production is performed by examining the reconstructed  $t\bar{t}$  invariant mass distribution resulting from a constrained kinematic fit to the  $t\bar{t}$  hypothesis.

Similar searches were performed at  $\sqrt{s} = 1.8 \text{ TeV}$  by the CDF and DØ collaborations during Run I of the Tevatron collider, finding no evidence for a  $t\bar{t}$  resonance. The resulting limits on  $\sigma_X \times B(X \rightarrow t\bar{t})$ , where  $\sigma_X$  is the resonance production cross section, were used to exclude a leptophobic  $Z'$  boson with  $\Gamma_{Z'} = 0.012M_{Z'}$ . The excluded mass regions at 95% C.L. are, respectively,  $M_{Z'} < 560 \text{ GeV}$  [3] and  $M_{Z'} < 480 \text{ GeV}$  [4].

## II. DØ DETECTOR

The Run II DØ detector is comprised of the following main components: the central tracking system, the liquid-argon/uranium calorimeter, and the muon spectrometer.

The central tracking system includes a silicon microstrip tracker (SMT) and a central fiber tracker (CFT), both located in a 2 T superconducting solenoid magnet. The SMT is designed to provide efficient tracking and vertexing capability at pseudorapidities of  $|\eta| < 3$  [5]. The system has a six-barrel longitudinal structure, each with a set of four layers arranged axially around the beampipe, and interspersed with 16 radial disks. A typical pitch of 50-80  $\mu\text{m}$  of the SMT strips allows a precision determination of the three-dimensional track impact parameter with respect to the primary vertex which is the key component of the  $b$ -tagging algorithm used in this analysis. The CFT has eight coaxial barrels, each supporting two doublets of overlapping scintillating fibers of 0.835 mm diameter, one doublet being parallel to the collision axis, and the other alternating by  $\pm 3^\circ$  relative to the axis [6].

The calorimeter is divided into a central section (CC) providing coverage out to  $|\eta| \approx 1$ , and two end calorimeters (EC) extending coverage to  $|\eta| \approx 4$  all housed in separate cryostats. Scintillators placed between the CC and EC provide sampling of showers at  $1.1 < |\eta| < 1.4$  [7].

The muon system, covering pseudorapidities of  $|\eta| < 2$ , resides beyond the calorimetry, and consists of three layers of tracking detectors and scintillating trigger counters. Moving radially outwards, the first layer is placed before the 1.8 T toroid magnets, and the two following layers are located after the magnets [8].

## III. EVENT SELECTION

The event selection in the  $e$ +jets and  $\mu$ +jets channel requires either an isolated electron with  $p_T > 20 \text{ GeV}$  and  $|\eta| < 1.1$ , or an isolated muon with  $p_T > 20 \text{ GeV}$  and  $|\eta| < 2.0$ . No additional leptons with  $p_T > 15 \text{ GeV}$  are allowed in the event. More details on the lepton identification as well as trigger requirements are reported elsewhere [9, 10]. In both channels, we require  $\cancel{E}_T$  to exceed 20 GeV and not be collinear with the lepton direction in the transverse plane. Jets are defined using a cone algorithm with radius  $\Delta\mathcal{R} = 0.5$  [11]. The selected events must contain four or more jets with  $p_T > 15 \text{ GeV}$  and rapidity  $|y| < 2.5$  [5], and must have the constrained kinematic fit described in Sect. V converge.

In order to improve the signal-to-background ratio, at least one jet is required to be identified as a  $b$ -jet. The lifetime based tagging algorithm used relies on the presence in the jet of a secondary vertex significantly displaced from the primary interaction vertex. Secondary vertices are reconstructed from two or more tracks satisfying the following requirements:  $p_T > 1$  GeV,  $\geq 1$  hit in the SMT layers, impact parameter significance  $d_{ca}/\sigma_{d_{ca}} > 3.5$  [12] and not be identified as arising from  $K_S^0$  or  $\Lambda$  decays or from  $\gamma$  conversions. If the secondary vertex reconstructed within a jet has a decay length significance  $L_{xy}/\sigma_{L_{xy}} > 7$  [13], the jet is tagged as a  $b$ -jet.

#### IV. MONTE CARLO SIMULATION

Monte Carlo (MC) samples corresponding to resonant  $t\bar{t}$  production are generated with PYTHIA 6.202 [14], using CTEQ5L [15] as the set of parton distribution functions, for ten different choices of the resonance mass  $M_X$ : 350 GeV, 400 GeV, 450 GeV, 500 GeV, 550 GeV, 600 GeV, 650 GeV, 750 GeV, 850 GeV, and 1000 GeV. In all cases, the width of the resonance is set to  $\Gamma_X = 0.012M_X$ . This qualifies  $X$  as a narrow resonance since its width is smaller than the expected mass resolution of the DØ detector (about  $0.04 M_X$  in Run I). This particular choice of  $\Gamma_X$  was made in order to compare the results to those quoted in Refs. [3, 4]. The generated resonance is forced to decay into  $t\bar{t}$  and only the events with one  $W$  boson decaying leptonically (including  $W \rightarrow \tau\nu$ ) and the other  $W$  boson decaying hadronically are selected for further processing through the detector simulation and reconstruction chain.

All MC samples for the background processes,  $t\bar{t}$  and  $W$ +jets, are generated using ALPGEN 1.3.3 [16] for the hard interaction. For subsequent generation of parton shower, hadronization and hadron decays PYTHIA 6.202 is used. The set of parton distribution functions used in both generators is CTEQ5L [15]. The  $W$ +jets samples have been generated separately for the various combinations of flavored quarks:  $Wjjjj$ ,  $Wcjjj$ ,  $Wbbjj$ , and  $Wccjj$ , where  $j$  denotes any of  $u, d, s$  quark or gluon.

In the generation of both resonant and non-resonant  $t\bar{t}$  production, a top quark mass  $m_t = 175$  GeV is assumed. All generated events have been processed through the full GEANT-based [17] DØ detector simulation and the same reconstruction program used for data.

#### V. RECONSTRUCTION OF THE $t\bar{t}$ INVARIANT MASS DISTRIBUTION

The  $t\bar{t}$  invariant mass is reconstructed using a constrained kinematic fit similar to the one used for the measurement of the top quark mass in Run I [18]. The lepton and jet resolutions used in the fit have been updated to reflect those of the Run II DØ detector. The following constraints are used in the fit:

- two jets must form the invariant mass of the  $W$  boson ( $M_W = 80.4$  GeV),
- the lepton and the  $\cancel{E}_T$ , taking into account the longitudinal neutrino momentum, must form the invariant mass of the  $W$  boson,
- the masses of the two reconstructed top quarks have to be equal, and are set to 175 GeV.

Only the four highest  $p_T$  jets are considered in the kinematic fit. From the resulting twelve possible jet-parton assignments, the one with the lowest  $\chi^2$  is chosen. This is found to give the correct solution in about 65% of the  $t\bar{t}$  events. In the current version of the analysis, the  $b$ -tagging information has not been used to reduce the number of possible jet permutations.

The expected  $t\bar{t}$  invariant mass distribution for resonance masses of 400 GeV and 750 GeV are illustrated in Figure 1.

#### VI. BACKGROUND ESTIMATION

Before  $b$ -tagging, the main background is  $W$ +jets, where the  $W$  boson decays leptonically. In most cases, the jets accompanying the  $W$  boson originate from light ( $u, d, s$ ) quarks and gluons, and only  $\sim 20\%$  of events with  $\geq 4$  jets in the final state contain at least one jet resulting from the fragmentation of a heavy ( $b$  or  $c$ ) quark. The next largest contribution is SM  $t\bar{t}$  production, followed by multijet production, with one of the jets misidentified as a lepton and accompanied by large  $\cancel{E}_T$  resulting from mismeasurements of jet energies. A significantly smaller contribution results from electroweak production of a single top quark. Backgrounds resulting from diboson ( $WW, WZ$  and  $ZZ$ ) as well as  $Z/\gamma^*$  production are estimated to be negligible and are not considered in this analysis. After  $b$ -tagging, only  $\sim 4\%$  of  $W$ +jets but  $\sim 60\%$  of  $t\bar{t}$  events remain, which makes SM  $t\bar{t}$  production become the dominant background in this analysis.

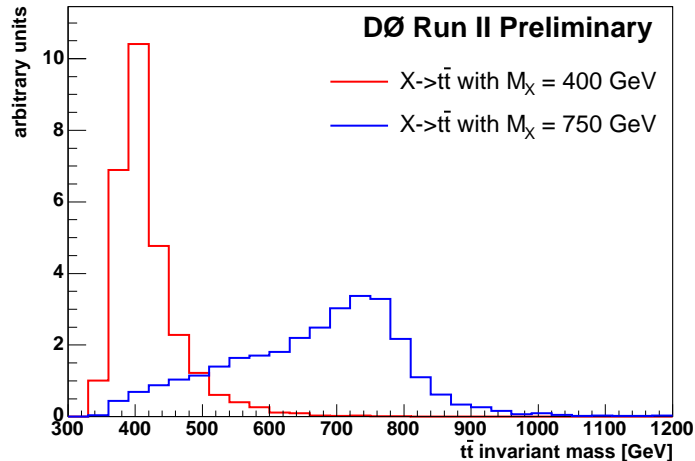


FIG. 1: Comparison of the expected  $t\bar{t}$  invariant mass distribution for a narrow-width resonance with mass  $M_X = 400$  GeV and  $M_X = 750$  GeV.

The SM  $t\bar{t}$  background is estimated by making use of the MC simulation, both to predict the total acceptance as well as the shape of the  $t\bar{t}$  invariant mass distribution. In the evaluation of the acceptance, event trigger, reconstruction and tagging efficiencies measured in data are taken into account. The tagging probability for each event is estimated by applying the tagging rates measured in data (tag rate functions) to each jet in the simulation, taking into consideration its flavor,  $p_T$ , and  $y$ . Finally, the expected yield is normalized to the SM theoretical prediction for the  $t\bar{t}$  production cross section:  $\sigma_{t\bar{t}} = 6.77 \pm 0.42$  pb for  $m_t = 175$  GeV [19].

The  $W$ +jets background is estimated from a combination of data and MC information. The expected number of  $W$ +jets events in the tagged sample is computed as the product of the estimated number of  $W$ +jets before tagging and the expected average event tagging probability. The former is obtained from the estimated number of events with real leptons in data, computed using the method described in Ref. [9] (Matrix Method) and after subtraction of the expected contributions from SM  $t\bar{t}$  and single top production. The latter is obtained by combining the  $W$ +jets flavor fractions estimated from MC with the event tagging probability, estimated from tagging rates measured in data, for each flavor configuration. The estimated composition of the  $W$ +jets background after the event selection, but before requiring at least one  $b$ -tag can be found in Table I. The shape of the reconstructed  $t\bar{t}$  invariant mass distribution is obtained from the MC simulation.

$Wjjjj$	$Wcjjj$	$W(b\bar{b})Jjj$	$W(c\bar{c})Jjj$	$Wb\bar{b}Jj$	$Wc\bar{c}Jj$
80.0%	4.8%	2.8%	4.9%	2.9%	4.5%

TABLE I: Expected fraction of each  $W$ +jets flavor type after preselection for both channels.  $j$  is any of u,d,s,g and  $J$  is any of u,d,s,c,g partons.  $WQ\bar{Q} + X$  ( $Q = b, c$ ) processes with only one reconstructed heavy quark jet are denoted as  $W(Q\bar{Q}) + X$ .

The multijet background is completely determined from data. The total number of expected events is estimated by applying the Matrix Method on the tagged sample. This method allows to determine the total normalization for this background source but, due to the limited available statistics, not the shape of the reconstructed  $t\bar{t}$  invariant mass distribution, which is derived from a larger sample of events with the lepton failing the strict isolation requirements and without requiring  $b$ -tagging. The kinematic biases resulting from the  $b$ -tagging requirement are mimicked by folding per-jet tag rate functions measured in data.

A summary of the prediction for the different background contributions in the combined  $\ell$ +jets channels, along with the observed number of events in data, is given in Table II.

	Number of events
$t\bar{t} \rightarrow \ell+\text{jets}$	$65.9 \pm 12.3$
$W+\text{jets}$	$15.3 + 3.0 - 6.6$
Multijet	$5.2 \pm 1.8$
$t\bar{t} \rightarrow \ell\bar{\ell}+\text{jets}$	$1.4 \pm 0.4$
single top	$1.4 \pm 0.3$
Total expected	$89.2 + 11.8 - 13.3$
Observed	108

TABLE II: Predicted and observed number of tagged events in the  $\ell+\text{jets}$  channels. Errors on the predictions include statistical and systematic uncertainties.

## VII. SYSTEMATIC UNCERTAINTIES

This analysis relies on the prediction of the overall normalization as well as the shape of the reconstructed  $t\bar{t}$  invariant mass distribution for both signal and the different backgrounds. The systematic uncertainties can be classified as those affecting only normalization and those affecting both normalization and shape of the  $t\bar{t}$  invariant mass distribution for one or more processes (signal or backgrounds).

The systematic uncertainties affecting only the normalization include e.g. the experimental uncertainties on the MC-to-data correction factors, the theoretical uncertainty on the SM prediction for  $\sigma_{t\bar{t}}$  (6%) [19] and  $\sigma_{single\,top}$  (12%) [20] and the uncertainty on the integrated luminosity (6.5%) [21].

The systematic uncertainties affecting the shape of the  $t\bar{t}$  invariant mass distribution in addition to the normalization have been studied both on signal and background samples. These include e.g. uncertainties on the jet energy calibration, jet reconstruction efficiency and  $b$ -tagging parameterizations for  $b$ ,  $c$  and light jets. The top quark mass is known with limited accuracy and thus contributes a systematic uncertainty: it enters the kinematic fit as a constraint ( $m_t = 175$  GeV) and thus affects the shape of the  $t\bar{t}$  invariant mass distribution; it also affects the normalization due to the mass-dependence of  $\sigma_{t\bar{t}}$ . To study the resulting systematic effect,  $t\bar{t}$  MC samples with  $m_t = 170$  GeV and  $m_t = 180$  GeV, normalized to the corresponding theoretical prediction ( $\sigma_{t\bar{t}} = 7.91$  pb and 5.80 pb, respectively), have been used. The difference in the total acceptance for different top quark mass values has also been included in the systematic uncertainty from this source.

The systematic uncertainties associated with the estimation of the fractions for the different flavor components of the  $W+\text{jets}$  background have been taken into account as well as the uncertainty associated with the modeling of the SM  $t\bar{t}$  background, in particular, gluon radiation effects. The latter is estimated by comparing the prediction from the nominal leading-order (LO)  $t\bar{t}$  sample with a sample built as an admixture of  $t\bar{t}$  and  $t\bar{t}+\text{jet}$  generated with LO MC, weighted according to the LO cross sections.

Finally, the most precise estimation of the tagged  $W+\text{jets}$  background would require to subtract the contribution from each hypothesized signal from the estimated number of  $W+\text{jets}$  before tagging. This has not been done in the current analysis but a conservative one sided systematic uncertainty ( $\sim 38\%$ ) on the predicted  $W+\text{jets}$  background has been included.

Table III gives a summary of the relative systematic uncertainties on the total SM background expectation for the combined  $\ell+\text{jets}$  channels. The effect of the different systematic uncertainties on the shape of the  $t\bar{t}$  invariant mass distribution can not be inferred from this table, but is included in the analysis.

## VIII. RESULT

After all selection cuts, 57 events remain in the  $e+\text{jets}$  channel and 51 events in the  $\mu+\text{jets}$  channel. Figure 2 shows the  $t\bar{t}$  invariant mass for the combined  $\ell+\text{jets}$  channels for the selected events in data and for the SM background predictions (see Sect. VI).

Assessment of the probability for known sources to reproduce the data is still being worked on. Assuming there is no resonance signal, a Bayesian approach is used to calculate 95% C.L. upper limits on  $\sigma_X \times B(X \rightarrow t\bar{t})$  for each hypothesized  $M_X$  discussed in Sect. IV. A Poisson distribution is assumed for the number of observed events in each bin, as well as flat prior probabilities for the signal cross section. Systematic uncertainties on the signal acceptance and background yields are implemented via a convolution procedure of a multivariate Gaussian distribution implementing a full covariance matrix including correlations.

The expected and observed 95% C.L. upper limits on  $\sigma_X \times B(X \rightarrow t\bar{t})$  as a function of  $M_X$  are summarized in Table IV and displayed in Fig. 3. This figure also includes the predicted  $\sigma_X \times B(X \rightarrow t\bar{t})$  for a leptophobic  $Z'$  boson

source	rel. syst. uncertainty (%)	
	$\sigma^+$	$\sigma^-$
Top quark mass (includes effect on $\sigma_{t\bar{t}}$ )	+8.7	-7.6
Signal subtraction from W+jets background estimate	+0.0	-6.6
Jet reconstruction	+5.6	-6.9
Luminosity	+4.6	-4.6
Theoretical uncertainty on $\sigma_{t\bar{t}}$	+4.2	-4.2
W+jets flavor composition	+2.9	-3.0
Jet energy calibration	+2.7	-3.2
b-tagging rate	+2.6	-2.6
MC-to-data correction factors	+2.5	-2.5
Theoretical uncertainty on $\sigma_{single\ top}$	+0.2	-0.2
Total	+13.2	-14.8

TABLE III: Summary of the relative systematic uncertainties on the overall normalization of the SM background.

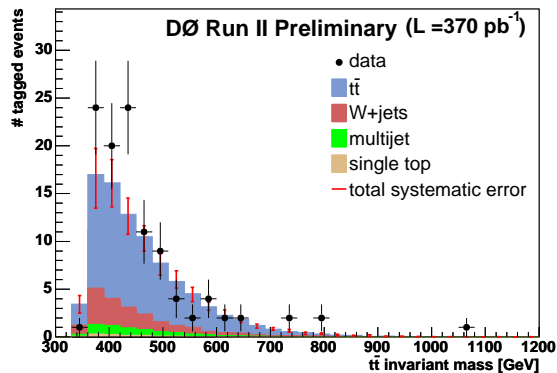


FIG. 2: The resulting  $t\bar{t}$  invariant mass distribution for the combined  $\ell$ +jets channels. The error bars drawn on top of the SM background indicate the total systematic uncertainty, which has significant bin-to-bin correlations.

with  $\Gamma_{Z'} = 0.012M_{Z'}$  which, combined with the experimental limits, allows to exclude  $M_{Z'} < 680$  GeV at 95% C.L.. This measurement extends the D0 Run I exclusion on  $M_{Z'}$  [3] by 120 GeV.

$M_X$ [GeV]	exp. limit [pb]	obs. limit [pb]
350	3.33	5.08
400	2.99	6.22
450	2.78	6.45
500	2.22	2.35
550	1.75	1.20
600	1.34	1.05
650	1.19	0.88
750	1.01	1.05
850	1.00	1.15
1000	1.17	1.43

TABLE IV: Expected and observed limits for  $\sigma_X \times B(X \rightarrow t\bar{t})$  at the 95% C.L. with systematic uncertainties taken into account.

## IX. CONCLUSION

A search for a narrow width resonance in the  $\ell$ +jets final states has been performed using data corresponding to an integrated luminosity of about  $370 \text{ pb}^{-1}$ , collected with the D0 detector during Run II of the Tevatron collider.

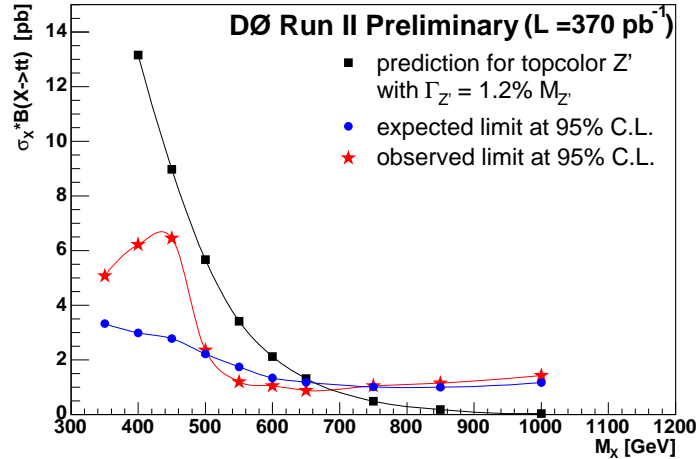


FIG. 3: Expected and observed 95% C.L. upper limits on  $\sigma_X \times B(X \rightarrow t\bar{t})$  compared with the predicted topcolor-assisted technicolor cross section for a  $Z'$  boson with a width of  $\Gamma_{Z'} = 0.012M_{Z'}$  as a function of resonance mass  $M_X$ .

By analyzing the reconstructed  $t\bar{t}$  invariant mass distribution and using a Bayesian method, model independent upper limits on  $\sigma_X \times B(X \rightarrow t\bar{t})$  have been obtained for different hypothesized masses of a narrow-width heavy resonance decaying into  $t\bar{t}$ . Within a topcolor-assisted technicolor model, the existence of a leptophobic  $Z'$  boson with  $M_{Z'} < 680$  GeV and width  $\Gamma_{Z'} = 0.012M_{Z'}$  can be excluded at 95% C.L..

#### Acknowledgments

We thank the staffs at Fermilab and collaborating institutions, and acknowledge support from the DOE and NSF (USA); CEA and CNRS/IN2P3 (France); FASI, Rosatom and RFBR (Russia); CAPES, CNPq, FAPERJ, FAPESP and FUNDUNESP (Brazil); DAE and DST (India); Colciencias (Colombia); CONACyT (Mexico); KRF (Korea); CONICET and UBACyT (Argentina); FOM (The Netherlands); PPARC (United Kingdom); MSMT (Czech Republic); CRC Program, CFI, NSERC and WestGrid Project (Canada); BMBF and DFG (Germany); SFI (Ireland); Research Corporation, Alexander von Humboldt Foundation, and the Marie Curie Program.

- 
- [1] C. T. Hill and S. Parke, Phys. Rev. D **49**, 4454 (1994).
  - [2] R. M. Harris, C. T. Hill and S. Parke, hep-ph/9911288 (1999).
  - [3] DØ Collaboration, V.M. Abazov *et al.*, Phys. Rev. Lett. **92**, 221801 (2004).
  - [4] CDF Collaboration, T. Affolder *et al.*, Phys. Rev. Lett. **85**, 2062 (2000).
  - [5] Rapidity  $y$  and pseudorapidity  $\eta$  are defined as functions of the polar angle  $\theta$  and parameter  $\beta$  as  $y(\theta, \beta) \equiv \frac{1}{2} \ln [(1 + \beta \cos \theta)/(1 - \beta \cos \theta)]$  and  $\eta(\theta) \equiv y(\theta, 1)$ , where  $\beta$  is the ratio of a particle's momentum to its energy.
  - [6] DØ Collaboration, V. Abazov *et al.*, in preparation for submission to Nucl. Instrum. Methods Phys. Res. A; T. LeCompte and H.T. Diehl, "The CDF and DØ Upgrades for Run II", Ann. Rev. Nucl. Part. Sci. **50**, 71 (2000).
  - [7] DØ Collaboration, S. Abachi *et al.*, Nucl. Instrum. Methods Phys. Res. A **338**, 185 (1994).
  - [8] V. Abazov *et al.*, FERMILAB-PUB-05-034-E (2005).
  - [9] DØ Collaboration, V. Abazov *et al.*, hep-ex/0504043.
  - [10] DØ Collaboration, V. Abazov *et al.*, hep-ex/0504058.
  - [11] We use the iterative, seed-based cone algorithm including midpoints, as described on p. 47 in G. C. Blazey *et al.*, in Proceedings of the Workshop: "QCD and Weak Boson Physics in Run II", edited by U. Baur, R. K. Ellis, and D. Zeppenfeld, FERMILAB-PUB-00-297 (2000).
  - [12] Impact parameter is defined as the distance of closest approach ( $d_{ca}$ ) of the track to the primary vertex in the plane transverse to the beamline. Impact parameter significance is defined as  $d_{ca}/\sigma_{d_{ca}}$ , where  $\sigma_{d_{ca}}$  is the uncertainty on  $d_{ca}$ .
  - [13] Decay length  $L_{xy}$  is defined as the distance from the primary to the secondary vertex in the plane transverse to the beamline. Decay length significance is defined as  $L_{xy}/\sigma_{L_{xy}}$ , where  $\sigma_{L_{xy}}$  is the uncertainty on  $L_{xy}$ .
  - [14] T. Sjostrand *et al.*, Comp. Phys. Commun. **135**, 238 (2001).

- [15] H. L. Lai *et al.*, Eur. Phys. J. **C12**, 375 (2000).
- [16] M.L. Mangano *et al.*, JHEP **07**, 001 (2003).
- [17] R. Brun and F. Carminati, CERN Programming Library Long Writeup **W5013** (1993).
- [18] DØ Collaboration, B. Abbot *et al.*, Phys. Rev. D **58**, 052001 (1998); DØ Collaboration, S. Abachi *et al.*, Phys. Rev. Lett. **79**, 1197 (1997).
- [19] R. Bonciani *et al.*, Nucl. Phys. B **529**, 424 (1998); M. Cacciari *et al.*, JHEP **0404**, 068 (2004); N. Kidonakis and R. Vogt, Phys. Rev. D **68**, 114014 (2003); N. Kidonakis and R. Vogt, Eur. Phys. J., C **33**, 466 (2004).
- [20] M. C. Smith and S. Willenbrock, Phys. Rev. D **54**, 6696 (1996); T. Stelzer *et al.*, Phys. Rev. D **56**, 5919 (1997).
- [21] T. Edwards *et al.*, FERMILAB-TM-2278-E (2004).